



## Deactivation resistance of Pd/Au nanoparticle catalysts for water-phase hydrodechlorination

Kimberly N. Heck<sup>a</sup>, Michael O. Nutt<sup>a</sup>, Pedro Alvarez<sup>b</sup>, Michael S. Wong<sup>a,c,d,\*</sup>

<sup>a</sup> Department of Chemical and Biomolecular Engineering, Rice University, 6100 S. Main Street, Houston, TX 77005, United States

<sup>b</sup> Department of Civil and Environmental Engineering, Rice University, 6100 S. Main Street, Houston, TX 77005, United States

<sup>c</sup> Department of Chemistry, Rice University, 6100 S. Main Street, Houston, TX 77005, United States

<sup>d</sup> Center of Biological and Environmental Nanotechnology, Rice University, 6100 S. Main Street, Houston, TX 77005, United States

### ARTICLE INFO

#### Article history:

Received 6 May 2009

Revised 24 July 2009

Accepted 27 July 2009

Available online 9 September 2009

#### Keywords:

Palladium

Gold

Nanoparticles

Groundwater

Trichloroethene

Remediation

Sulfide

Chloride

Deactivation

### ABSTRACT

Palladium-decorated gold nanoparticles (Pd/Au NPs) have recently been shown to be highly efficient for trichloroethene hydrodechlorination, as a new approach in the treatment of groundwater contaminated with chlorinated solvents. Problematically, natural groundwater can contain chloride and sulfide ions, which are known poisons in Pd-based catalysis. In this study, the effects of chloride and sulfide on the trichloroethene hydrodechlorination catalytic activity were examined for non-supported Pd/Au NPs and Pd NPs, and alumina-supported Pd (Pd/Al<sub>2</sub>O<sub>3</sub>). Over the concentration range of 0–0.02 M NaCl, the catalytic activity of Pd/Au NPs was unaffected, while the activities of both the Pd NPs and Pd/Al<sub>2</sub>O<sub>3</sub> catalysts dropped by ~70%. Pd/Au NPs were found to be highly resistant to sulfide poisoning, deactivating completely at a ratio of sulfide to surface Pd atom (S:Pd<sub>surf</sub>) of at least 1, compared to Pd NPs deactivating completely at a ratio of 0.5. Pd/Al<sub>2</sub>O<sub>3</sub> retained activity at a ratio of 0.5, pointing to a beneficial role of the Al<sub>2</sub>O<sub>3</sub> support. Sulfide poisoning of Pd/Au NPs with different Pd surface coverages provided a way to assess the nature of active sites. The gold component was found to enhance both Pd catalytic activity and poisoning resistance for room-temperature, water-phase trichloroethene hydrodechlorination.

© 2009 Elsevier Inc. All rights reserved.

### 1. Introduction

Chlorinated ethenes constitute a class of volatile organic compounds considered to be some of the most harmful groundwater contaminants. These compounds and their isomers are probable human carcinogens, have been linked to liver damage, nervous system damage, and lung damage, and, with extreme exposure, can cause death in humans [1]. One of the most prevalent of these compounds is trichloroethene (TCE) [2], which has also been found at 832 of 1430 National Priority List Superfund sites at concentrations far above the US EPA maximum containment level of 5 ppb [3]. Still used as a metal degreaser and in textile manufacture, TCE ranks 16th on the Comprehensive Environmental Response and Compensation Liability Act of 2005 (CERCLA) priority list of hazardous compounds [4]. It also shows up in groundwater as a result of biotic degradation of perchloroethene. TCE is particularly threatening if left untreated, as it will degrade through natural

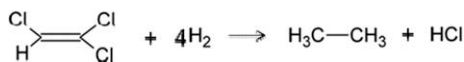
attenuation to vinyl chloride [4,5], the 4th most hazardous substance on the CERCLA list [4].

We recently reported on the high efficiency of palladium-decorated gold nanoparticles (Pd/Au NPs) for the catalytic room-temperature, water-phase hydrodechlorination (HDC) of TCE into ethane (Scheme 1) [6,7]. We characterized Pd/Au NPs to have a Pd-shell/Au-core structure using a combination of UV–vis spectroscopy, X-ray photoelectron spectroscopy, and reaction rate data [7], with recent extended X-ray absorption spectroscopy results showing that the Pd/Au NPs have a surface that is enriched in Pd atoms, *i.e.*, the NPs have a Au core with Pd on the surface [9] (Fang et al., in preparation). The Pd/Au NP catalytic activity was directly controlled by the Pd metal surface coverage of the 4-nm Au NPs. A maximum rate (~1800 L/g<sub>Pd</sub>/min) was found near 70% surface coverage, nominally 100× higher than Pd/Al<sub>2</sub>O<sub>3</sub> (~12 L/g<sub>Pd</sub>/min). Observed for some other catalytic reactions, Au promotes Pd metal for TCE HDC catalytic activity possibly by creating a Pd–Au interface as population of active sites, by inducing the formation of Pd surface ensembles as the active sites, or by modifying the electronic structure of the Pd metal [8].

Toward their application to real groundwater systems, the long-term durability of the Pd/Au NP catalysts needs to be addressed with regard to catalyst deactivation. Groundwater typically

\* Corresponding author. Address: Department of Chemical and Biomolecular Engineering, Rice University, 6100 S. Main Street, Houston, TX 77005, United States. Fax: +1 713 348 5478.

E-mail address: [mswong@rice.edu](mailto:mswong@rice.edu) (M.S. Wong).



Scheme 1. TCE HDC reaction.

contains a multitude of substances which could impact Pd/Au NP catalytic performance [10–12]. Perhaps the most pertinent to address are chloride ( $\text{Cl}^-$ ) and hydrosulfide ( $\text{SH}^-$ , “sulfide” for short) ions, where the former can be found at concentrations ranging from 1.0 to 1000 mg/L and the latter can be produced naturally from native anaerobic bacteria. Both chemical species are known to adsorb onto Pd surfaces [13–16] and to reduce Pd activity [17–28]. The rapid poisoning of Pd-based catalysts during aqueous-phase hydrodechlorination by sulfide ions is a well-known problem [18,29–31]. In this work, we studied the effects of sulfide and chloride ions on TCE HDC reaction rates of Pd/Au NPs, observing that chloride had no effect and sulfide had a markedly less effect compared to Pd NPs and Pd/ $\text{Al}_2\text{O}_3$ . We performed catalytic titration experiments using sulfide as the poison to gain insights into the nature of the active sites for TCE HDC sites.

## 2. Experimental

### 2.1. Preparation of Pd/Au NPs and Pd NPs

The Pd/Au NPs were prepared as previously reported [7]. Briefly, 1 mL of a gold salt solution (1 wt% = 25 mM; prepared by adding 1 g of  $\text{HAuCl}_4 \cdot 3\text{H}_2\text{O}$  (99.99%, Sigma-Aldrich) to 99 g of deionized  $\text{H}_2\text{O}$ ) was added to 79 mL of deionized  $\text{H}_2\text{O}$ . A second solution of 0.04 g of tannic acid, 0.05 g of trisodium citrate, and 0.0173 g of  $\text{K}_2\text{CO}_3$  in 20 mL of deionized water was also prepared. Both solutions were heated to 60 °C, and then the tannic acid solution was added rapidly to the gold salt solution under vigorous stirring. The solution immediately turned reddish brown, indicating the formation of Au NPs. The temperature of the solution was increased until boiling, and allowed to boil for 25 min. Finally, the solution (calculated particle concentration of  $2.9 \times 10^{15}$  NP/L) was removed from the heat source and stored in a separate container.

For the Pd coatings, a specified amount (15–60  $\mu\text{L}$ ) of a 2.4-mM  $\text{H}_2\text{PdCl}_4$  solution (prepared from 0.0426 g of  $\text{PdCl}_2$  (99.99%, Sigma-Aldrich) dissolved in 100 mL deionized water and 480  $\mu\text{L}$  1 M HCl solution) was mixed with 2 mL of the as-synthesized Au NP sol. The resulting solution was then bubbled with hydrogen gas (99.999%, Matheson) for two min. After bubbling, the solution was aged in a sealed vial overnight at room temperature prior to use. Assuming complete reduction of Au and Pd ions into metal, 15, 30, and 60  $\mu\text{L}$  of Pd salt solution yielded Pd/Au NPs containing 3.5, 6.8, and 12.8 wt% Pd, respectively. They, respectively, correspond to 4-nm Au NPs with 15%, 30%, and 60% of monolayer (ML) coverage by Pd metal atoms (Table 1). The particle size of 4 nm was derived from transmission electron microscopy analysis as we reported previously [7].

The Pd NPs were prepared using the same procedure for Au NP synthesis, except for the Au salt solution was replaced by 10.4 mL

of a  $\text{H}_2\text{PdCl}_4$  solution (2.4 mM) combined with 69.6 mL of  $\text{H}_2\text{O}$  [7]. A dark coffee-brown sol containing 4-nm Pd NPs (calculated particle concentration of  $2.9 \times 10^{15}$  NP/L) was the result. A Pd/ $\text{Al}_2\text{O}_3$  (1 wt% Pd) catalyst was purchased from Sigma-Aldrich, and was used as is.

### 2.2. Catalyst testing

#### 2.2.1. Reactor set-up

The catalytic testing of the NPs was conducted similar to our previous studies [6,7]. Batch reactors were prepared by adding 168.6–172.5 mL of  $\text{H}_2\text{O}$  (so as to keep the volume constant at 173 mL after the addition of the catalyst sol/suspension) and a stir bar to a 250-mL, Teflon-sealed glass bottle. The bottles were sealed with a cap outfitted with a rubber septum, and sparged with  $\text{H}_2$  gas for 15 min to saturate the  $\text{H}_2\text{O}$  and fill the headspace. TCE was then added (3  $\mu\text{L}$ , 99.5%, Aldrich), resulting in a liquid concentration of approximately 43 ppm (43 mg/L, 325  $\mu\text{M}$ ), far below the saturation concentration of 1200 ppm at 25 °C. Pentane (0.2  $\mu\text{L}$ , 99.7%, Burdick & Jackson) was added as an internal standard for gas-chromatography (GC) headspace analysis. The reactors were stirred rapidly for at least 3 h or until the measured concentrations showed no change over time, indicating total dissolution of the TCE and pentane and the establishment of vapor–liquid equilibrium.

#### 2.2.2. Reaction analysis

The catalyst was used directly without purification and introduced into the reactor via syringe injection of an aliquot of sol (containing Pd/Au or Pd NPs) or suspension (containing Pd/ $\text{Al}_2\text{O}_3$ ). For GC headspace analysis, 100- $\mu\text{L}$  aliquot samples of the headspace gas in the batch reactor were withdrawn with a gas-tight syringe and injected into an Agilent Technologies 6890 GC equipped with a flame ionization detector (FID) and a packed column (6-in  $\times$  1/8-in outer diameter) containing 60/80 Carboxpack B/1% SP-1000 (Supelco). Calibration curves were prepared for chlorinated ethenes, chlorinated ethanes, and ethane.

The pH of the reaction medium was monitored using pH paper (Whatman Panpeha pH indicator strips, Sigma-Aldrich) before injection of the catalyst and at the end of the reaction. At complete conversion of TCE, the pH should drop to a value of 3.1 theoretically, due to HCl formation. For all catalyst samples tested, *i.e.*, Pd/Au NPs, Pd NPs, and Pd/ $\text{Al}_2\text{O}_3$ , for both chloride and sulfide testing studies, the initial reactor pH was  $\sim$ 6.0 and the final pH was  $\sim$ 5.5. This slight pH decrease, as observed by others [18,32], indicates that the reaction system has some buffering capacity that limits pH change. The Pd and Pd/Au NP reaction systems contain small amounts of citrate, carbonate, and tannic acid, which are buffering ions. In the Pd/ $\text{Al}_2\text{O}_3$  case, the alumina support could buffer the solution around its point-of-zero charge (generally between pH 6.4 and 9.5) [33].

#### 2.2.3. Testing of chloride effect

Prior to charging with  $\text{H}_2$ , TCE, pentane, and catalyst, solutions of 1 M NaCl (prepared from 5.84 g 99.99% NaCl (Fisher) and 100 mL deionized water) were added to the reactor such that the

**Table 1**  
Pd content of catalytic materials tested, and amounts charged to reactor.

Catalyst nanomaterials tested		Pd weight loading (wt% Pd)	Estimated Pd dispersion (%Pd surface atoms)	Calculated amount of surface Pd atoms, charged to reactor (nmol)
Pd/Au NPs	15% ML	3.55	100	72
	30% ML	6.85	100	72
	60% ML	12.4	100	72
Pd NPs		100	34.7	89.2
Pd/ $\text{Al}_2\text{O}_3$		1	21 <sup>a</sup>	493

<sup>a</sup> Taken from Ref. [32].

total reaction volume (accounting for the eventual added catalyst sol/suspension) was 173 mL, giving final concentrations ranging from 0 to 0.02 M chloride. The following catalyst aliquots were injected: 2 mL of the 30%-Pd/Au NP sol; 1 mL of the Pd NP sol combined with 1 mL of H<sub>2</sub>O; and 25 mg of Pd/Al<sub>2</sub>O<sub>3</sub> suspended in 2 mL of H<sub>2</sub>O.

#### 2.2.4. Testing of sulfide effect

Hereafter, the term “sulfide” refers to the hydrosulfide ion, the dissociated form of hydrogen sulfide (H<sub>2</sub>S ↔ H<sup>+</sup> + SH<sup>-</sup>, pK<sub>a</sub> = 7.05 at 20 °C [34]). A sulfide solution (0.01 M) was prepared by dissolving 0.0211 g Na<sub>2</sub>S·9H<sub>2</sub>O (98%, Sigma-Aldrich) in 8.78 mL deionized water (Na<sub>2</sub>S + H<sub>2</sub>O ↔ 2Na<sup>+</sup> + SH<sup>-</sup> + OH<sup>-</sup>), and was combined with catalyst sol/suspensions before injection.

For Pd/Au NP sols, 4 mL of 15%-Pd/Au NPs, 2 mL of 30%-Pd/Au NPs, or 0.5 mL of 60%-Pd/Au NPs (Table 1) was treated with 0–13 μL of the sulfide solution, to vary the sulfide:surface Pd atom (S:Pd<sub>surf</sub>) ratio from 0 to 1.8. Pd NP sol (1 mL) was diluted with 1 mL of H<sub>2</sub>O (so as to keep the final liquid volume in the reactor constant at 173 mL), and treated with 0–9.0 μL of sulfide solution to vary the sulfide:surface Pd atom (S:Pd<sub>surf</sub>) ratio from 0 to 1. Similarly, a Pd/Al<sub>2</sub>O<sub>3</sub> suspension (25 mg powder in 2 mL of H<sub>2</sub>O) was treated with 0–49 μL of sulfide solution. All suspensions were stirred briefly then left unstirred at room temperature for at least 3 h prior to injection. The total reaction volume was 173 mL.

The concentrations of surface Pd atoms in the reactor after catalyst injection were 0.42 μM, 0.51 μM, and 2.85 μM for the Pd/Au NPs, Pd NPs, and Pd/Al<sub>2</sub>O<sub>3</sub> catalysts, respectively. For Pd and Pd/Au NPs [7], the magic cluster structural model was used [35–38] and the complete reduction of the gold and palladium precursor salts was assumed. We estimate that each of the nanoparticle sols contains 2.91 × 10<sup>15</sup> NPs/L. For the Pd NPs, we assume that the surface atoms are contained only in the 7th shell, and hence the concentration of surface Pd in the sol is 88 μM. In the case of the bimetallic Pd–Au NPs, if the added Pd is assumed to constitute a partial 8th shell around the Au NP, we estimate that it covers approximately 15–60% of the Au NP surface, resulting in a surface Pd concentration of 18–72 μM. The amount of surface Pd on the Pd/Al<sub>2</sub>O<sub>3</sub> sample was estimated using the literature reported metal dispersion of 21% [32], which indicates a surface concentration of 210 μg of surface Pd per gram of Pd/Al<sub>2</sub>O<sub>3</sub>.

#### 2.2.5. Testing the effect of adding Au NPs to Pd/Au NPs

To study the effects of adding Au NPs on sulfide deactivation of Pd/Au NPs, 1–3 mL of the Au NP sol was mixed with 2 mL of the Pd/Au NPs prepared with 30 μL of H<sub>2</sub>PdCl<sub>4</sub> (to get 30%-Pd/Au NPs) before adding 2.4 μL of the sulfide solution.

### 3. Results and discussion

#### 3.1. Determination of reaction rate constant

Reaction rate constants for the conversion of TCE by Pd-based catalysts have generally been assumed to be pseudo first order in TCE concentration, and zero order in H<sub>2</sub> concentration (from very high H<sub>2</sub> concentrations) [6,7,32]:

$$-\frac{dC_{\text{TCE}}}{dt} = k_{\text{meas}} C_{\text{TCE}}$$

where the fitted first-order rate constant  $k_{\text{meas}} = k_{\text{obs}} \times C_{\text{cat}}$ , where  $k_{\text{obs}}$  (units of L/g<sub>Pd</sub>/min) is the rate constant normalized by the amount of catalyst present, and  $C_{\text{cat}}$  and  $C_{\text{TCE}}$  are the concentrations of the catalyst and TCE, respectively. Accounting for exposed Pd atoms, initial turnover frequency values can be calculated as  $\text{TOF} = -k_{\text{obs}} \times C_{\text{TCE},0} \times \text{Pd atomic weight} \div \text{Pd dispersion}/60$ . It is noted that

$k_{\text{obs}}$  is equivalent to  $-(dC_{\text{TCE}}/dt)_0/C_{\text{cat}}/C_{\text{TCE},0}$ , where  $C_{\text{TCE},0}$  is the initial TCE concentration.

As previously reported, Pd/Au NPs catalyze TCE HDC with a first-order dependence on TCE concentration [6,7]. Fig. 1a shows Pd/Au NPs with 30% Pd coverage exhibiting this first-order dependence, in the absence and presence of additional chloride. The first-order rate constants are listed out in Table 2. However, the monometallic Pd NPs and Pd/Al<sub>2</sub>O<sub>3</sub> catalysts did not show this behavior (Fig. 1b and c). TCE conversions were linear with time, indicating zero-order dependence on TCE concentration; conversions leveled off above a conversion of ~80%.

According to the studies by Kopinke et al. [12], Reinhard and coworkers [32], and us [6], Pd/Al<sub>2</sub>O<sub>3</sub> catalysts were reported to be first order in TCE. By running the reaction for a longer period of time in this work, however, we observed clearly and reproducibly the non-first-order dependence on TCE. We found that the reaction rates for Pd NPs and Pd/Al<sub>2</sub>O<sub>3</sub> catalysts were first order at low TCE concentrations (<1 ppm, close to the 1 ppm used by Kopinke et al. [12] and by Reinhard and coworkers [32]) and non-first-order at high TCE concentrations (29 ppm, as used in this study) [39]. An interesting implication is that the higher TCE concentrations lead to competitive chemisorption of TCE on the active sites of Pd NPs and Pd/Al<sub>2</sub>O<sub>3</sub> catalysts, which does not happen with Pd/Au NPs.

Since rate constants for catalysts exhibiting different rate laws cannot be compared, we chose to compare initial reaction rates and initial TOF values instead (Table 2). Whereas the TOF's for Pd/Au NPs were derived from initial reaction rates via the first-order rate constants, the TOF's for the pure Pd-based catalysts were derived in a different manner. The initial reaction rate of the monometallic Pd catalysts was characterized as

$$-\left(\frac{dC_{\text{TCE}}}{dt}\right)_0 / C_{\text{cat}} = -r'_{\text{TCE}}$$

where  $-r'_{\text{TCE}}$  (units of mol-TCE/g<sub>Pd</sub>/min) is the initial slope of the first 3–4 data points of a TCE concentration–time profile divided by Pd catalyst reactor charge amount. Accounting for exposed Pd atoms, initial turnover frequency values were then calculated as  $\text{TOF} = -r'_{\text{TCE}} \times \text{Pd atomic weight} \div \text{Pd dispersion}/60$ , which is equivalent to the TOF definition given earlier for Pd/Au NPs.

#### 3.2. Effect of chloride on the rate of HDC reaction

As shown in Fig. 1 and Table 2, the activity of the Pd/Al<sub>2</sub>O<sub>3</sub> and Pd NPs fell drastically with increasing chloride concentration, decreasing as much as 30% of its original activity at the highest chloride concentration used. This chloride effect is seen in other catalytic systems, such as both gas-phase oxidation [23–26] and gas- and liquid-phase HDC [27,28] reactions. In gas-phase HDC, HCl formed as a byproduct of the reaction and inhibited the activity by reversibly competing with the chlorinated reactant for active sites [28,32]. In water-phase HDC, this species may play a similar inhibitory role [27].

In contrast to our observations with Pd/Al<sub>2</sub>O<sub>3</sub> and Pd NPs, Lowry and Reinhard reported that a chloride concentration of 0.028 M had no effect on activity on the aqueous-phase HDC of TCE over a Pd/Al<sub>2</sub>O<sub>3</sub> catalyst [18]. This difference could be attributed to the higher pH of 9.6 used by Lowry and Reinhard compared to the lower pH used in our reaction system (i.e., initial pH of 6, lowering to 5.5 by the end of the reaction). The higher pH values led to increased Pd/Al<sub>2</sub>O<sub>3</sub>-catalyzed TCE HDC rates, which could have masked the chloride inhibitory effect we observed [18].

A reasonable explanation for the deactivation of the pure Pd catalysts (Pd NPs and Pd/Al<sub>2</sub>O<sub>3</sub>) is the chemisorption of chloride to the Pd surface. In an electrochemical study of halide adsorption at Pd electrodes, Soriaga and coworkers showed that chloride can

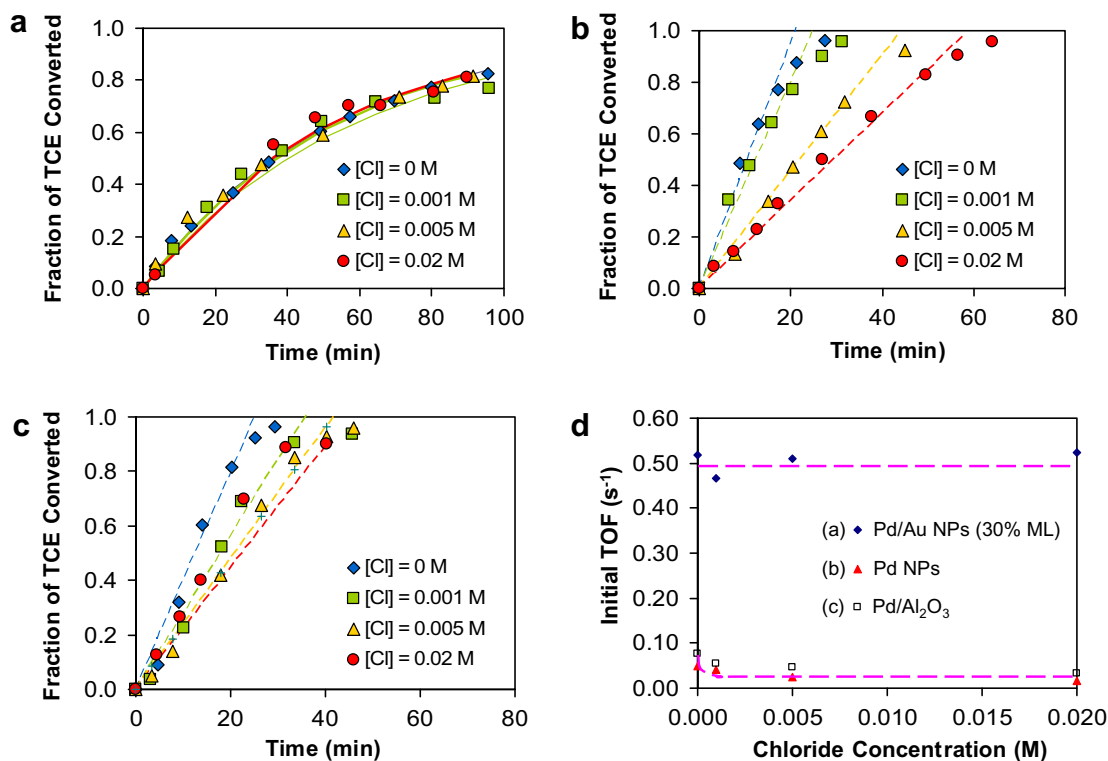


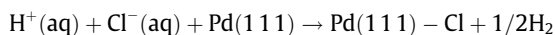
**Fig. 1.** Fractional conversion of TCE vs. time for (a) Pd/Au NPs (30% ML), (b) Pd NPs, and (c) Pd/Al<sub>2</sub>O<sub>3</sub> at various chloride concentrations. Points are experimental results. Solid lines in panel (a) are first-order best fits, and dashed lines in panels (b) and (c) show initial slopes used to determine initial TCE HDC activity. (d) Initial turnover frequencies at different chloride concentrations, with dashed lines drawn to guide the eye.

**Table 2**

Parameters and results from chloride poisoning studies for 30%-Pd/Au NPs, Pd NPs, and Pd/Al<sub>2</sub>O<sub>3</sub>. Reaction conditions: C<sub>TCE,0</sub> = 221 μM, room temperature.

Catalyst	Reactor chloride concentration (mmol/L)	First-order rate constant $k_{obs}$ (L/g <sub>Pd</sub> /min)	Initial rate $-r'_{TCE} \times 10^{-3}$ (mol-TCE/g <sub>Pd</sub> /min)	Initial turnover frequency TOF (mol-TCE/mol-Pd <sub>surf</sub> /s)
Pd/Au NPs (30% ML)	0	900	292.5	0.52
	1	809	262.9	0.47
	5	885	287.6	0.51
	20	907	294.7	0.52
Pd NPs	0	–	28.1	0.050
	1	–	23.5	0.042
	5	–	13.3	0.024
	20	–	9.9	0.018
Pd/Al <sub>2</sub> O <sub>3</sub>	0	–	42.7	0.076
	1	–	30.0	0.052
	5	–	25.8	0.045
	20	–	18.3	0.031

oxidatively adsorb to Pd(111) crystals under acidic conditions via the reaction [40]



The amount of Cl added to the reactors was far in excess of the amount of surface Pd atoms, and so by way of the law of mass action, the amount of chlorine surface species would also increase if there was sufficient amount of hydronium ions H<sup>+</sup>(aq). Acid and neutral pH conditions would favor chlorine surface species formation (leading to greater susceptibility to catalyst deactivation and lower HDC rates) and basic pH would disfavor chlorine surface species formation (leading to catalyst deactivation resistance and higher HDC rates). From *in situ* surface-enhanced Raman spectroscopic investigations, we were recently able to detect surface-bound chlo-

rine atoms on Pd–Au catalytic surfaces in the closely related reaction of 1,1-dichloroethylene HDC [41].

Whereas Pd-only catalysts deactivated significantly, the activity of the Pd/Au NPs unexpectedly remained constant and unaffected by Cl concentration at the same condition of near-neutral pH (Fig. 1a and d), suggesting that the extent of chlorine surface species formation on the Pd metal was lowered in the presence of Au. This reduced binding affinity to chlorine atoms may be correlated to the increased d-band electron density of Pd caused by the Au, as previously observed through X-ray photoelectron spectroscopy [7].

### 3.3. Effect of sulfide on the rate of HDC reaction

Fig. 2 and Table 3 show the results for the sulfide poisoning experiments on monometallic Pd and Pd/Au NP (30% ML) catalyst,

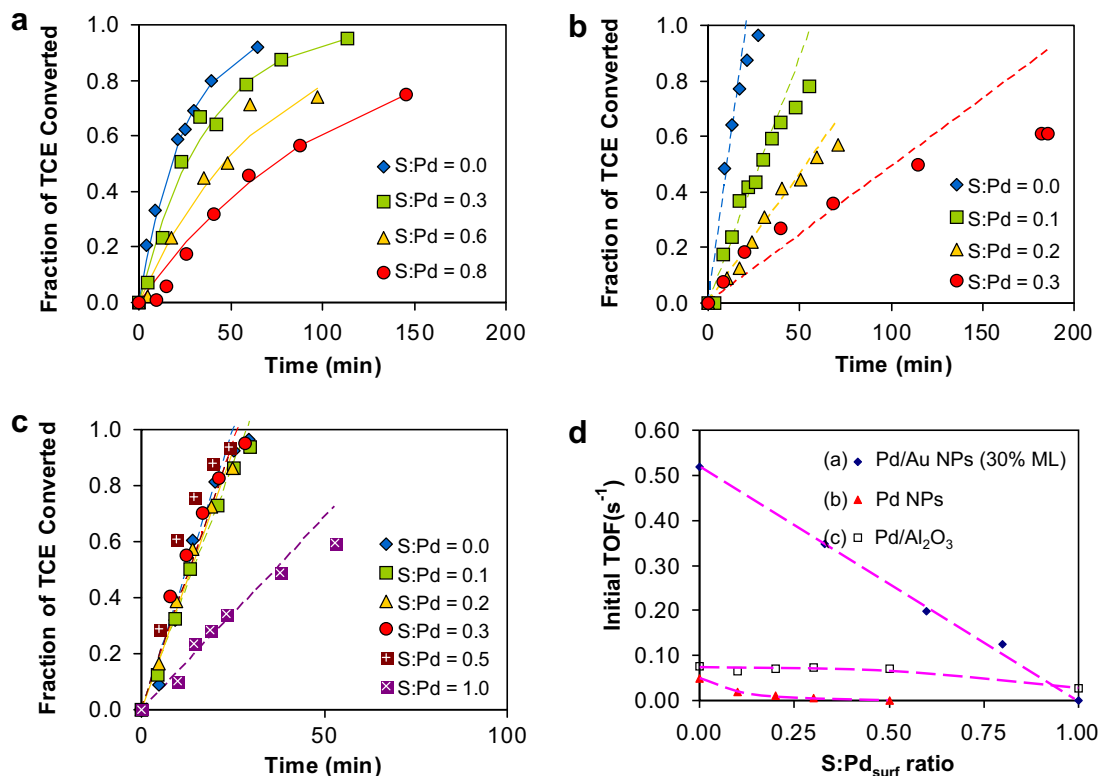


**Fig. 2.** Fractional conversion of TCE vs. time for (a) Pd/Au NPs (30% ML), (b) Pd NPs, and (c) Pd/Al<sub>2</sub>O<sub>3</sub> at various S:Pd<sub>surf</sub> ratios. Points are experimental results. Solid lines in panel (a) are first-order best fits, and dashed lines in panels (b) and (c) show initial slopes used to determine initial TCE HDC activity. (d) Initial turnover frequencies with S:Pd<sub>surf</sub> ratio, with dashed lines drawn to guide the eye.

**Table 3**

Parameters and results from sulfide poisoning experiments for 30%-Pd/Au NPs, Pd NPs, and Pd/Al<sub>2</sub>O<sub>3</sub>. Reaction conditions: C<sub>TCE,0</sub> = 221 μM, room temperature.

Catalyst	Sulfide added (μg)	S:Pd <sub>surf</sub> molar ratio	First-order rate constant $k_{obs}$ (L/g <sub>Pd</sub> /min)	Initial rate $-r'_{TCE} \times 10^{-3}$ (mol-TCE/g <sub>Pd</sub> /min)	Initial turnover frequency TOF (mol-TCE/mol-Pd <sub>surf</sub> /s)
Pd/Au NPs (30% ML)	0	0.0	900.4	292.5	0.52
	0.76	0.33	604.9	196.6	0.35
	1.39	0.6	342	111.2	0.20
	1.85	0.8	215	69.88	0.12
	2.31	1.0	0	0	0
Pd NPs	0	0.0	–	28.1	0.050
	0.29	0.1	–	10.4	0.018
	0.57	0.2	–	5.47	0.010
	0.85	0.3	–	2.88	0.005
	1.43	0.5	–	0	0
Pd/Al <sub>2</sub> O <sub>3</sub>	0	0.0	–	42.7	0.076
	1.58	0.1	–	37.4	0.066
	3.16	0.2	–	39.8	0.071
	4.74	0.3	–	40.9	0.072
	7.90	0.5	–	40.6	0.072
	15.8	1	–	14.7	0.026

in which sulfide-to-surface Pd atom ratios were considered. In the absence of sulfide, the activity measured for the control catalysts had initial TOF values of 0.076 and 0.050 mol-TCE/mol-Pd<sub>surf</sub>/s for the Pd/Al<sub>2</sub>O<sub>3</sub> and Pd NP catalysts, respectively. The Pd/Au NP catalyst had an initial TOF 0.52 mol-TCE/mol-Pd<sub>surf</sub>/s, in agreement with our earlier work (which used a higher initial TCE concentration of 7 μL compared to 3 μL used in this study) [7].

TCE HDC activity of the Pd/Au NP and Pd NP catalysts monotonically decreased with added sulfide, while added sulfide had little effect on the Pd/Al<sub>2</sub>O<sub>3</sub> catalyst until S:Pd<sub>surf</sub> ratio of 1. The latter observation could be due to the Al<sub>2</sub>O<sub>3</sub> support material. Al<sub>2</sub>O<sub>3</sub> has

been studied for its use as a gas-phase adsorbent of sulfide and other sulfur containing compounds, where the adsorption is theorized to occur either to strong Lewis acid sites of the Al<sub>2</sub>O<sub>3</sub> or to surface hydroxyl groups via hydrogen bonding.[42–45] While there are no data available for the aqueous-phase adsorption of sulfide, it is feasible that all of the sulfide could have been adsorbed to the Al<sub>2</sub>O<sub>3</sub>. If each sulfide atom (the ionic radius of sulfide is 1.84 Å → cross-sectional area of 10.63 Å<sup>2</sup>) populates an amount of area on the support (BET surface area of Pd/Al<sub>2</sub>O<sub>3</sub> = 155 m<sup>2</sup>/g [32]) equal to its cross-sectional area, then 25 mg of catalyst would have a monolayer adsorption sulfide capacity of 2.19 mmoles,



which is six orders of magnitude greater than the largest sulfide amount added to the Pd/Al<sub>2</sub>O<sub>3</sub> catalyst in our batch studies (i.e., 0.49  $\mu$ L–4.9 nmoles of sulfide).

The deactivation of Pd NPs by sulfide could be analyzed more quantitatively. Complete deactivation observed at a S:Pd<sub>surf</sub> ratio of 0.5, suggesting that 2 Pd atoms are involved in the HDC reaction. This ratio is close to those found from STM and EXAFS studies of H<sub>2</sub>S on Pd surfaces, in which surface saturation corresponded to a S:Pd<sub>surf</sub> ratio of 0.43 (=3 S atoms chemisorbed on 7 Pd atoms [14–16]) for Pd(111) and 0.50 for Pd(001) [13]. The rapid decrease in TCE HDC reaction rate with sulfide content indicated preferential adsorption on Pd atoms of highest activity, which are often correlated to atoms with the lowest coordination number [13,46].

Interestingly, the Pd/Au NP catalyst deactivated more slowly than the Pd NPs and Pd/Al<sub>2</sub>O<sub>3</sub>. This material did not fully deactivate until a S:Pd<sub>surf</sub> ratio one of  $\sim$ 1 was reached (Fig. 2d). The Au apparently enhances the sulfide poisoning resistance of Pd for TCE HDC. This beneficial presence of Au was seen in gas-phase hydrodesulfurization thiophene using alloyed Pd–Au/Al<sub>2</sub>O<sub>3</sub> catalysts by Venezia et al. [47,48], for which it was concluded that Au prevented the bulk formation of catalytically inactive Pd<sub>4</sub>S crystallites.

#### 3.4. Effect of adding Au NPs to Pd/Au NPs for TCE HDC

We considered explaining the enhanced deactivation resistance the result of adsorption of sulfide onto the exposed Au surface of Pd/Au NPs. Lambert and coworkers showed that Pd atoms form two- and three-dimensional islands on Au(111) at room temperature at low (7%) and high (70%) Pd coverages, respectively, to leave

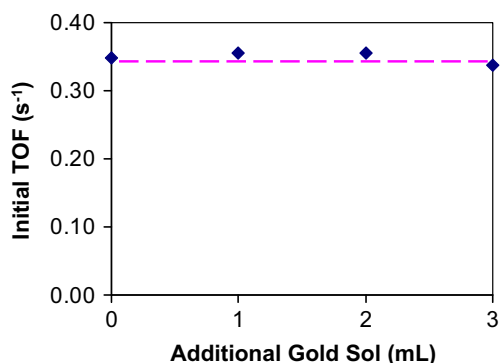


Fig. 3. Measured initial turnover frequencies for 30% Pd/Au NPs as a function of additional Au NPs. The amount of sulfur S:Pd<sub>surf</sub> ratio was set at 0.3. Line drawn to guide the eye.

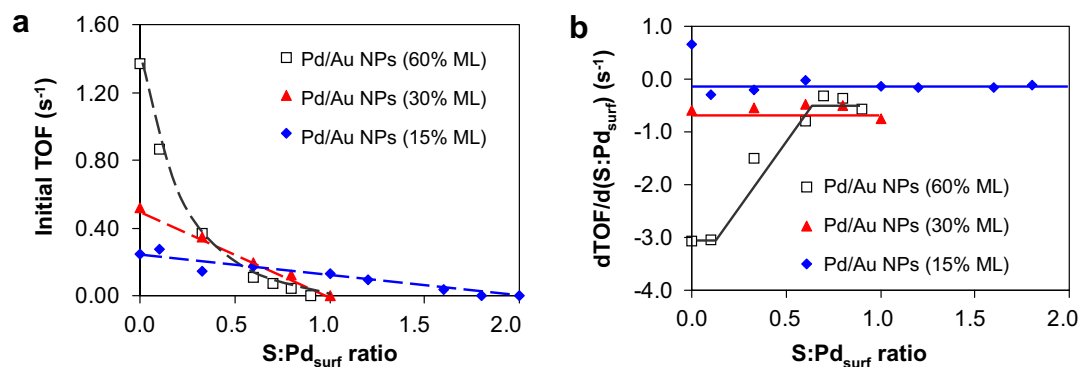


Fig. 4. (a) TOF values and (b) rates of TOF change with sulfur amount (calculated using 3-point numerical differentiation) for Pd/Au NPs with varying Pd surface coverages, as a function of S:Pd<sub>surf</sub> ratio. Lines are drawn to guide the eye.

the underlying Au uncovered [49,50]. It is well known that sulfide compounds bind to Au surfaces [47,48,51,52]. Wierse et al. reported that sulfide ions can adsorb weakly onto Au surfaces in water up to surface saturation coverages of 0.5–0.6 S:Au<sub>surf</sub> [52]. Adsorption onto any exposed Au would reduce the sulfide amount available to bind to the presumed Pd-based active sites.

To test this idea, we combined varying amounts of gold-only NPs to the Pd/Au NPs (30% ML) prior to the sulfide treatment step, and determined the reaction rate constants of the resulting NP mixtures. From Fig. 3, it can be seen that the rate constants did not change when Au NPs were added, indicating that the sulfide ions did not adsorb onto the Au NP surfaces. Otherwise, the rate constants were expected to increase as increasing amounts of Au NPs removed the sulfide from solution. The non-effect of additional gold surface area indicated that the sulfide preferentially bonded to Pd-based sites (i.e., Pd atoms or Pd–Au mixed sites) over pure Au sites. According to Zhang et al., the Pd–S bond of thiol capped Pd NPs is shorter than the Au–S bond in thiol capped Au NPs, suggesting Pd–S bonding is stronger than Au–S bonding and therefore more preferred [53].

#### 3.5. Effect of Pd/Au NP composition

Sulfide deactivation experiments were carried out on Pd/Au NP catalysts with varying Pd surface coverages (Fig. 4a). Besides 30% ML coverage, 15% and 60% ML coverages were studied. All materials exhibited lowered reaction rates with added sulfide, but the deactivation characteristics differed. The 15% and 30% deactivated with a linear dependence on S:Pd<sub>surf</sub> ratio, and the much more active 60%-ML Pd/Au NPs deactivated much more rapidly at low S:Pd<sub>surf</sub> ratios. Complete deactivation occurred at S:Pd<sub>surf</sub> ratios of 1.8, 1.0, and 0.8 for 15%, 30%, and 60% ML coverages, respectively. The 15% ML samples were poisoned completely with twice the amount of sulfide per surface Pd atom, whereas the 30% and 60% ML samples were poisoned completely at the roughly the same sulfide level.

Analyzing the rate of deactivation change with S:Pd<sub>surf</sub> ratio provided additional insights into the sulfide poisoning effect (Fig. 4b). For the 30% ML material, the rate of TOF change was constant with increasing sulfide content (at a d(TOF)/d(S:Pd<sub>surf</sub>) value of  $\sim$ –0.57 s<sup>–1</sup>), which likely indicated the NP catalysts contained one population of active sites with equivalent catalytic activity. For the 15% ML material, the rate of TOF change was also constant at a lower value (with d(TOF)/d(S:Pd<sub>surf</sub>) =  $\sim$ –0.15 s<sup>–1</sup>), indicating that there was one population of active sites with equivalent catalytic activity and with less sensitivity to sulfides. This lower susceptibility to sulfide poisoning is consistent Pd/Au NPs (15% ML) complete deactivating at a S:Pd<sub>surf</sub> ratio that was nearly twice that

of Pd/Au NPs (30% ML). This also led to Pd/Au NPs (15% ML) becoming more active than Pd/Au NPs (30% ML) when S:Pd<sub>surf</sub> ratios exceeded ~0.60.

The 60% ML material showed a more complex rate of TOF change with sulfide content, in which  $d(\text{TOF})/d(\text{S:Pd}_{\text{surf}}) \approx -3.0 \text{ s}^{-1}$  at low S:Pd<sub>surf</sub> ratios and decreased to  $\sim -0.51 \text{ ds}^{-1}$  at high S:Pd<sub>surf</sub> ratios. This indicated the presence of more than one population of active sites on the catalyst surface, in which the highly active sites deactivated first in the presence of sulfides and the less active sites deactivated more slowly. These less active sites of the Pd/Au NPs (60% ML) could be equivalent to those of Pd/Au NPs (30% ML), based on the approximately similar rates of TOF change. Furthermore, the Pd/Au NPs (60% ML) did not contain the low-activity but more-deactivation-resistant active sites found in Pd/Au NPs (15% ML).

Sautet and coworkers conducted both theoretical and experimental studies on the dechlorination reaction of TCE over a model (110) PdCu catalyst, consisting of alternating rows of Pd and Cu at the surface [54,55]. It was shown that the carbon–carbon double bond preferentially adsorbed on two adjacent Pd sites, while the carbon–chloride bond cleavage was assisted by the Cu atoms, onto which chloride atoms preferentially remained. These studies underlined the importance of Pd and Cu adjacency in TCE dechlorination, in which mixed metal surface atoms behave as catalytically active sites.

While it cannot be separated from ensemble (clustering of atoms as active site), electronic (ligand), and geometric (e.g., strain, interatomic distance changes) effects, this mixed metal site effect could explain some of the poisoning trends of Pd/Au NPs with different Pd coverages. The 15%-ML material perhaps contains Pd metal in the form of isolated atoms or small two-dimensional Pd ensembles surrounded by Au atoms, which would not be found in the NPs with higher Pd content. These Pd atoms or small ensembles would have a large Pd–Au interface at which TCE HDC can occur and which sulfide can chemisorb and poison. The 30%-ML material contains no isolated Pd atoms but contains larger Pd ensembles such that its population of active sites is more active and more sensitive to sulfide poisoning, with the 60%-ML material containing even larger Pd ensembles. Baddeley et al. indicated that Pd atoms assembled into three-dimensional ensembles (2 atom layers thick) on a Au(111) surface at 70% monolayer coverage [49,50], suggesting that Pd/Au NPs (60% ML) could also contain 3-D Pd ensembles. We thus associate the population of highly active and sulfide-sensitive sites in this material to 3-D Pd ensembles and the less active and less sulfide-sensitive sites to smaller 2-D ensembles. The latter are found in the 30%-ML material but not in the 15%-ML one. It is presumed that the Pd-shell/Au-core nanostructure is retained and that these presumptive Pd ensembles do not rearrange during the reaction. While our results do not confirm these possibilities at this point, the technique of *in situ* extended X-ray absorption spectroscopy as applied to the room-temperature TCE HDC water-phase reaction catalyzed by “naked” nanoparticles will be very helpful for verification.

#### 4. Summary and conclusions

This study analyzed the poisoning effects of Pd/Al<sub>2</sub>O<sub>3</sub>, Pd NP, and Pd/Au NP catalysts for the aqueous-phase hydrodechlorination of trichloroethene. Pd NPs and Pd/Al<sub>2</sub>O<sub>3</sub> deactivated in the presence of chloride due to Cl chemisorption onto Pd active sites. In contrast, Pd/Au NPs did not deactivate, which was speculated to result from the electronic effect of Au on Pd. Pd/Al<sub>2</sub>O<sub>3</sub> catalyst showed little deactivation behavior in the presence of sulfides due to their interactions with the support; alumina can play an important role in mitigating sulfide poisoning when operating with real groundwater. The Pd NP catalyst became completely inactive at a S:Pd<sub>surf</sub> ratio

of 0.5, close to the reported surface saturation values for sulfide on Pd surfaces. The Pd/Au catalysts completely deactivated only at higher sulfide amounts, indicating a higher level of sulfide poisoning resistance. This improved sulfide resistance was not related to the well-known ability of Au to bind to sulfides and thiol compounds, but rather, to the formation of Pd–Au mixed metal active sites. The Pd content of the Pd/Au NPs controlled the type of active site populations on the particle surface. The NPs with a Pd coverage of 60% ML were the most active but they deactivated most rapidly, showing complete deactivation at S:Pd<sub>surf</sub> = 1. The least active NPs tested were those with a Pd coverage of 15% ML, which deactivated least rapidly, with complete deactivation at S:Pd<sub>surf</sub> of ~2. These Pd/Au NPs can be the basis for highly active and highly stable catalysts for groundwater treatment applications.

#### Acknowledgments

This work is supported by NSF (IGERT, DGE-0504425; CBEN, EEC-0647452), the Welch Foundation (C-1676) and SABIC Americas. We acknowledge helpful discussions with Mr. Y.-L. Fang and Mr. R. J. Smith.

#### References

- [1] N.C.f.E. Assessment, Sources, Emission, and Exposure for Trichloroethylene (TCE) and Related Chemicals, US Environmental Protection Agency, Washington, DC, 2001.
- [2] J.S. Zogorski, J.M. Carter, T. Ivahnenko, W.W. Lapham, M.J. Moran, B.L. Rowe, P.J. Squillace, P.L. Toccalino, The quality of our nation's waters: Volatile organic compounds in the nation's ground water and drinking-water supply wells; Circular 1292. US Geological Survey, Reston, VA, 2006.
- [3] National Primary Drinking Water Regulations, United States Environmental Protection Agency, 1995.
- [4] ASTDR, Top 20 Hazardous Substances, 2005.
- [5] Y.J. An, D.H. Kampbell, J.W. Weaver, J.T. Wilson, S.W. Jeong, Environ. Pollut. 130 (2004) 325–335.
- [6] M.O. Nutt, J.B. Hughes, M.S. Wong, Environ. Sci. Technol. 39 (2005) 1346–1353.
- [7] M.O. Nutt, K.N. Heck, P. Alvarez, M.S. Wong, Appl. Catal. B 69 (2006) 115–125.
- [8] B.G. Ponec V, Catalysis by Metals and Alloys, Elsevier, 1995.
- [9] M.S. Wong, P.J.J. Alvarez, Y.-L. Fang, N. Akcin, M.O. Nutt, J.T. Miller, K.N. Heck, J. Chem. Technol. Biotechnol. 84 (2009) 158–166.
- [10] C. Schuth, N.A. Kummer, C. Weidenthaler, H. Schad, Appl. Catal. B-Environ. 52 (2004) 197–203.
- [11] W.W. McNab, R. Ruiz, M. Reinhard, Environ. Sci. Technol. 34 (2000) 149–153.
- [12] F.D. Kopinke, K. Mackenzie, R. Kohler, Appl. Catal. B 44 (2003) 15–24.
- [13] D. Burgler, G. Tarrach, T. Schaub, R. Wiesendanger, H.J. Guntherodt, Phys. Rev. B 47 (1993) 9963–9966.
- [14] V.R. Dhanak, A.G. Shard, B.C.C. Cowie, A. Santoni, Surf. Sci. 410 (1998) 321–329.
- [15] J.G. Forbes, A.J. Gellman, J.C. Dunphy, M. Salmeron, Surf. Sci. 279 (1992) 68–78.
- [16] M.E. Grillo, C. Stampfl, W. Berndt, Surf. Sci. 317 (1994) 84–98.
- [17] B. Coq, G. Ferrat, F. Figueras, J. Catal. 101 (1986) 434–445.
- [18] G.V. Lowry, M. Reinhard, Environ. Sci. Technol. 34 (2000) 3217–3223.
- [19] C.G. Schreier, M. Reinhard, Chemosphere 31 (1995) 3475–3487.
- [20] M.N. Berube, B. Sung, M.A. Vannice, Appl. Catal. 31 (1987) 133–157.
- [21] J. Sepulveda, N. Figoli, React. Kinet. Catal. Lett. 53 (1994) 155–160.
- [22] P.C. Largentiere, N.S. Figoli, J. Chem. Technol. Biotechnol. 48 (1990) 361–368.
- [23] D.O. Simone, T. Kennelly, N.L. Brungard, R.J. Farrauto, Appl. Catal. 70 (1991) 87–100.
- [24] B. Miranda, E. Diaz, S. Ordenez, A. Vega, F.V. Diez, Appl. Catal. B 64 (2006) 262–271.
- [25] D. Roth, P. Gelin, M. Primet, E. Tena, Appl. Catal. A 203 (2000) 37–45.
- [26] P. Marecot, A. Fakche, B. Kellali, G. Mabilon, M. Prigent, J. Barbier, Appl. Catal. 3 (1994) 283–294.
- [27] C.H. Xia, H. Xu, W.Z. Wu, X.M. Liang, Catal. Commun. 5 (2004) 383–386.
- [28] C.D. Thompson, R.M. Rioux, N. Chen, F.H. Ribeiro, J. Phys. Chem. B 104 (2000) 3067–3077.
- [29] N. Munakata, M. Reinhard, Appl. Catal. B 75 (2007) 1–10.
- [30] D. Angeles-Wedler, K. Mackenzie, F.-D. Kopinke, Environ. Sci. Technol. 42 (2008) 5734–5739.
- [31] M.G. Davie, H. Cheng, G.D. Hopkins, C.A. LeBron, M. Reinhard, Environ. Sci. Technol. 42 (2008) 8908–8915.
- [32] G.V. Lowry, M. Reinhard, Environ. Sci. Technol. 33 (1999) 1905–1910.
- [33] J. Park, J.R. Regalbutto, J. Colloid Interface Sci. 175 (1995) 239–252.
- [34] M.A.A. Schoonen, H.L. Barnes, Geochim. Cosmochim. Acta 52 (1988) 649–654.
- [35] T. Teranishi, M. Miyake, Chem. Mater. 10 (1998) 594–600.
- [36] L.N. Lewis, Chem. Rev. 93 (1993) 2693–2730.
- [37] J.M. Thomas, Pure Appl. Chem. 60 (1988) 1517–1528.
- [38] A.L. Mackay, Acta Crystallogr. 15 (1962) 916.
- [39] Y. Fang, K.N. Heck, P. Alvarez, M.S. Wong, in preparation.

- [40] A. Carrasquillo, J.J. Jeng, R.J. Barriga, W.F. Temesghen, M.P. Soriaga, *Inorg. Chim. Acta* 255 (1997) 249–254.
- [41] K.N. Heck, B.G. Janesko, G.E. Scuseria, N.J. Halas, M.S. Wong, *J. Am. Chem. Soc.* 130 (2008) 16592–16600.
- [42] R.W. Glass, R.A. Ross, *J. Phys. Chem.* 77 (1973) 2576–2578.
- [43] A. Ionescu, A. Allouche, J.P. Aycard, M. Rajzmann, F. Hutschka, *J. Phys. Chem. B* 106 (2002) 9359–9366.
- [44] Y. Okamoto, M. Ohhara, A. Maezawa, T. Imanaka, S. Teranishi, *J. Phys. Chem. C* 100 (1996) 2396–2407.
- [45] O. Saur, T. Chevreau, J. Lamotte, J. Travert, J.C. Lavalley, *J. Chem. Soc.-Faraday Trans. I* 77 (1981) 427–437.
- [46] G. Somorjai, *Introduction to Surface Chemistry and Catalysis*, Wiley Interscience, New York, 1994.
- [47] A.M. Venezia, V. La Parola, V. Nicoli, G. Deganello, *J. Catal.* 212 (2002) 56–62.
- [48] A.M. Venezia, V. La Parola, G. Deganello, B. Pawelec, J.L.G. Fierro, *J. Catal.* 215 (2003) 317–325.
- [49] C.J. Baddeley, R.M. Ormerod, A.W. Stephenson, R.M. Lambert, *J. Phys. Chem.* 99 (1995) 5146–5151.
- [50] A.W. Stephenson, C.J. Baddeley, M.S. Tikhov, R.M. Lambert, *Surf. Sci.* 398 (1998) 172–183.
- [51] R.L. McCarley, Y.T. Kim, A.J. Bard, *J. Phys. Chem.* 97 (1993) 211–215.
- [52] D.G. Wierse, M.M. Lohrengel, J.W. Schultze, *J. Electroanal. Chem.* 92 (1978) 121–131.
- [53] P. Zhang, T.K. Sham, *Mater. Res. Soc. Symp. Proc.* 738 (2003) G.13.14.1.
- [54] Y. Jugnet, J.C. Bertolini, L. Barbosa, P. Sautet, *Surf. Sci.* 505 (2002) 153–162.
- [55] S. Barbosa, *J. Catal.* 207 (2002) 127–138.